



Shahid Chamran
University of Ahvaz

Journal of Applied and Computational Mechanics



Research Paper

Verification and Validation of a Network Algorithm for Single-phase Flow Modeling using Microfluidic Experiments

S.A. Filimonov¹, D.V. Guzei^{1,2}, A.S. Yakimov¹, A.I. Pryazhnikov¹, V.A. Zhigarev¹, A.V. Minakov^{1,2}

¹ Siberian Federal University, 79 Svobodny pr., Krasnoyarsk, 660041, Russian Federation,
Email: S.Filimonov@sfu-kras.ru (S.A.F.); A.Yakimov@sfu-kras.ru (A.S.Y.); APryazhnikov@sfu-kras.ru (A.I.P.); VZhigarev@sfu-kras.ru (V.A.Z.)

² Kutateladze Institute of Thermophysics, SB RAS, Novosibirsk, 630090, Russian Federation,
Email: DGuzey@sfu-kras.ru (D.V.G.); AMinakov@sfu-kras.ru (A.V.M.)

Received May 19 2023; Revised July 22 2023; Accepted for publication August 04 2023.

Corresponding author: D.V. Guzei (DGuzey@sfu-kras.ru)

© 2023 Published by Shahid Chamran University of Ahvaz

Abstract. This paper presents the results of the full-scale verification and validation of the mathematical model and numerical algorithm for the network computation of a single-phase flow in a highly branched pipeline chain. The essential difference of this work from others is that highly branched hydraulic networks with homogeneous and non-uniform permeability, containing more than 70 thousand branches, are considered. Such branched networks are important in many applications. Therefore, the development of algorithms for calculating flows in such networks is very important. The network model is based on hydraulic theory, and the numerical algorithm relies on the network analogue of the well-known control volume method. At the same time, obtaining reliable experimental data for testing models for calculating very branched hydraulic networks is very difficult. In this work, microfluidic technologies are used to solve this problem. Data of laboratory experiments, obtained using microfluidic models of branched networks with homogeneous and heterogeneous permeability, containing several tens of thousands of branches, as well as CFD simulation results in full 3D formulation employing the fine computational grids were used to validate the model. The Reynolds number ranged from 0.81 to 13. Conducted validation has shown a good qualitative and quantitative concordance of the results of network and hydrodynamic simulation, as well as the data of the microfluidic experiments. The error in determining the total pressure drop in the branched hydraulic network with heterogeneous permeability, containing 37,855 nodes and 74,900 branches, did not exceed 5%. It has been demonstrated that the speed of solving a single-phase flow problem in a highly branched chain using network simulation techniques is 60 times more of magnitude higher as compared to CFD simulation at virtually the same accuracy.

Keywords: Poro-network models, hydraulic networks, microfluidic chips, experiment, CFD, verification and validation.

1. Introduction

In the contemporary world, numerical simulation is practically irreplaceable when studying natural systems, as well as designing technical objects. Different simulation approaches are used when solving fluid dynamics problems depending on the type of an object (system, device, and so on). If an object can be represented in the form of a set of extended elements, in which the ratio of characteristic sizes differs in 10-1000 times, such as for example, pipelines, channels, gas ducts, etc., the network hydraulic simulation is usually used [1-3]. The computation of required characteristics of such system (pressure, velocity, temperature, etc.) is carried out using methods of hydraulic circuit theory (HCT) [1]. A hydraulic circuit consists of a set of nodes and branches, and as a rule, represents a simple oriented graph [4]. The mass and energy conservation laws (Kirchhoff's laws) are ensured in the nodes, and the momentum conservation law, which describes the pressure drop along the branch length depending on flow rate, is fulfilled in the branches. As a rule, such an approach is used for simulating large-scale objects, such as water supply systems, pipeline transport, and the like; that is, the size of the element of the system under study can reach several kilometers. Recently, however, network methods are increasingly used when simulating micro-scale systems. Looking carefully at the porous medium structure, one can see that the void space of some oil-bearing rocks is a branched network of microchannels with characteristic sizes ranged from 1 to 1000 μm , which allows using a network approach for their simulation [5, 6]. Moreover, the number of microchannels of the studied sample can reach several millions [7], and their total length can reach hundreds of kilometers.

Network models of pore space can be divided into two types: quasi-static and dynamic. Quasi-static models are based on the assumption that capillary forces dominate over viscous forces. This type models are used to determine the dependence of relative permeability and capillary pressure on the saturation state in the porous medium [8]. If the viscous forces are comparable to capillary forces, then a dynamic network model must be used, which takes into account the multiphase fluid motion and the hydraulic resistances, arising during this motion [9, 10]. In case of a single-phase flow, the network model of the pore space is strictly dynamic.



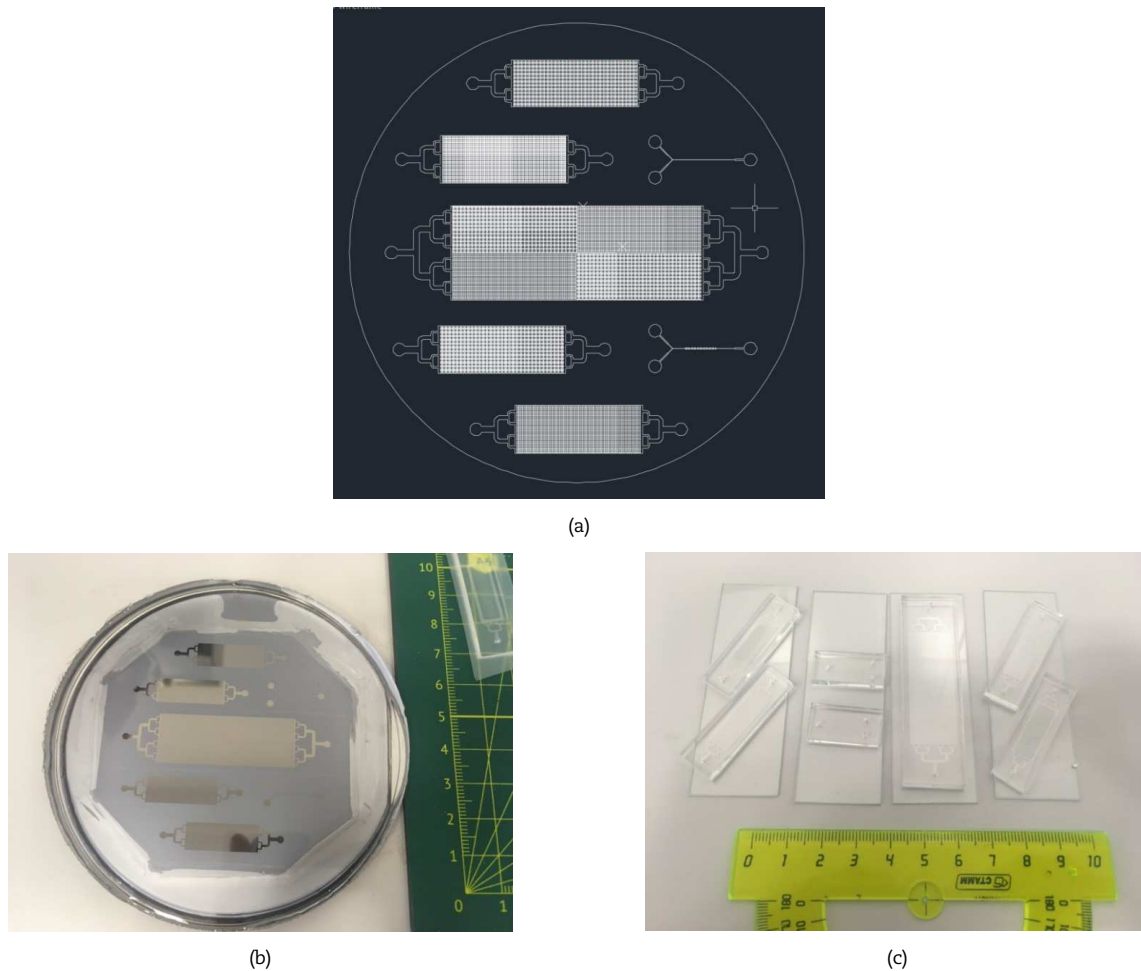


Fig. 1. PDMS microfluidic chip fabrication stages: (a) forming microfluidic chip topology; (b) silicon master mould; (c) sealed PDMS chips.

Recently, network models of pore space continue to develop. For example, models are emerging that take into account the transport of solid or colloidal particles [11], which can clog pores [12]. A particular area of developing multiphase fluid flow simulation in porous media is the coupling of one-dimensional (1D) network and spatial (2D, 3D) hydrodynamic models into a single hybrid model [13, 14]. Such approaches allow to circumvent the limitations of one-dimensional representation of a large complex object (e.g. a fracture in a rock) while maintaining acceptable computational speeds compared to a fully spatial model.

One of the main problems, when using network methods to simulate flow in microporous media, is verification, since it is impossible to locate flow rate and pressure sensors within the pore space ensuring their minimal influence on the flow. Therefore, as a rule, verification of computation results is carried out based on integral parameters, such as pressure drop in the sample or the amount of oil displaced from the sample over a given period of time [15]. The disadvantage of this approach is that it is impossible to observe fluid flow process inside the sample. Even an original validation method of network computations, such as comparison with an unsteady front motion pattern, obtained by X-ray imaging [16], although providing much more information, does not allow observing individual processes in each pore. Microfluidic chips [17] can be used to obtain a clear flow pattern without resorting to complex tools such as radiography [17-18]. At the same time, the topology of the microchip can reproduce the characteristics of a real rock [19]. To a large extent, the validation of modeling methods depends on the correct construction of the geometry of the object of study. For microporous systems, this is a separate challenge [20-22]. In our case, the use of a microchip with a previously known geometry allows us to avoid errors associated with its determination by indirect methods and focus directly on modeling techniques. Since fluid flow in the channels is strictly laminar, using direct numerical simulation, one can obtain an accurate flow pattern in each microchannel of the chip, which can subsequently be used to verify the network model.

The purpose of the present work was to carry out full-scale verification and validation of the mathematical model and numerical algorithm for network computation of a single-phase flow in a highly branched pipeline chain. The essential difference of this work from others is that highly branched hydraulic networks with homogeneous and non-uniform permeability, containing more than 70 thousand branches, are considered. Such branched networks are important in many applications. Therefore, the development of algorithms for calculating flows in such networks is very important. However, there are significant difficulties in obtaining reliable experimental data for such models. In our work, microfluidic technologies were used to test network hydraulic algorithms. The data of laboratory experiments, obtained using microfluidic models of branched networks with homogeneous and heterogeneous permeability, containing several tens of thousands of branches, as well as CFD simulation results, were used for validation. Validation of network hydraulic algorithms using microfluidic experiments for such a branched channel chain has not been done before.

2. Fabrication of Microfluidic Chip to Validate Network Method

To validate the numerical algorithms under development, the microchip topologies were designed (see Fig. 1a) and a master mould was fabricated for their casting from polydimethylsiloxane (PDMS). As reactive elastomer, PDMS has good resistance against liquid hydrocarbons and sufficient strength against destruction when pumping fluid. The master surface was made of



monocrystalline silicon, since the proper micromachining techniques are well developed, and it has low adhesion to PDMS, which allows forming very fine structures with an accuracy of 100 nm. The chips represent microfluidic chambers with a rectangular array of square columns. The distance between the columns is the same as the column facet length, namely, 25, 50, 75, and 100 μm. One chip has four areas, which are arranged in a staggered mode in chamber with arrays of 50 and 100 μm columns.

Fabricating microfluidic chips consists of two steps: forming a channelized surface on a wafer and covering the channelized surface with another wafer to create a closed capillary network with inlet and outlet interfaces for fluid delivery and discharge, as well as for connecting integrated modules. The choice of methods depends primarily on the materials used and their properties, as well as on the required precision of fabrication and other characteristics.

The designed topology was projected with accuracy of 1 μm onto a standard 3" silicon plate for photolithography, coated with positive photoresist, using a DWL 66fs maskless photolithographer (Heidelberg, Germany). Etching was performed employing a Plasmalab System 100 ICP 380 (Oxford instruments, UK) plasma chemical etching machine using the anisotropic reactive-ion etching method. Actual etch depth was 39.5–40.0 μm, which was evaluated using an Ambios XP-1 profilometer (Ambios Technology, USA). As a result, a silicon master mold was produced to cast chips with a set topology (see Fig. 1b) from PDMS with an accuracy of 1 μm. The chips were sealed using plasma activation in the original plasma treatment facility. For this purpose, the PDMS chip and the slide glass were treated in plasma for 120 seconds to form silanol groups on the surface. Further, the treated surfaces were brought into contact with each other so that adhesive bonding occurred. The chip was then incubated for 15 minutes at 125°C to catalyze the formation of siloxane bonds between the PDMS molecules and the glass. The finished products are shown in Fig. 1c.

3. Simulation Methodology for a Single-phase Flow in Microfluidic Chip

3.1 Network simulation methodology for a single-phase flow in microfluidic chip

A network model, based on hydraulic circuit theory, was developed to simulate a single-phase flow in highly branched hydraulic channels [1, 3]. When using the network approach, the microchip topology can be easily represented as a set of nodes and branches. To describe network model, we introduce the appropriate notations, namely, set of nodes is denoted as N , and set of branches (pipes) as U (see Fig. 2).

Let O_i be a subset of branches starting at the i -th node, and I_i be a subset of branches ending at the i -th node. Accordingly, each branch is associated with a pair of nodes with the adopted notation: N_{in} is the start node and N_{out} is the end node. The direction of the branch is set from the initial node to the final one; respectively, the flow rate q_l and velocity u_l on the l -th branch ($l \in U$) can take either a positive value (the fluid flow coincides with the direction of the branch) or a negative one. It is also worth noting that, in general, most nodes in the network are unconnected; on average, each node has two to four branches. Consequently, only a relatively small subset of existing branches needs to be identified from the whole set of branches $U_{i,j}$, where $i, j \in N$.

This approach allows specifying the coupling matrix for the whole graph in the form (1). Using this expression, the network flow distribution problem can be reduced to a combination of the mass conservation law in a node (2) and the resistance law in a pipe (3):

$$D_{il} = \begin{cases} 1, & \text{if } l \in O_i \\ -1, & \text{if } l \in I_i \\ 0, & \text{otherwise} \end{cases}, \tag{1}$$

$$\sum_{l \in U_i} D_{il} q_l = Q_i, \quad i \in N, \tag{2}$$

$$s_l |q_l| q_l = \sum_{i \in N} D_{il} \cdot p_{Di} \pm P_c, \quad l \in U, \tag{3}$$

where q_l is the carrying flow in the branch, Q_i is the mass source existing at the node, p_{Di} is the pressure in the i -th node, P_c is the capillary pressure, whose sign depends on the distribution in the pipe, s_l is the drag coefficient, determined by the formula known also as Darcy-Weisbach equation:

$$s_l = \left(\frac{\lambda_{fr} \cdot l}{d} + \xi \right) \frac{\rho}{2 \cdot f^2}, \tag{4}$$

where λ_{fr} is the linear friction coefficient, d is the hydraulic diameter of the branch, l is the branch length, ρ is the liquid density, f is the pipe cross-section area, ξ is the local drag coefficient.

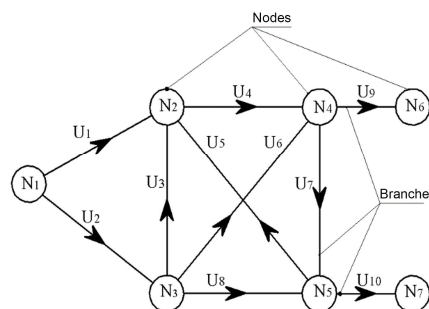


Fig. 2. Example of an oriented graph Nodes Branches.



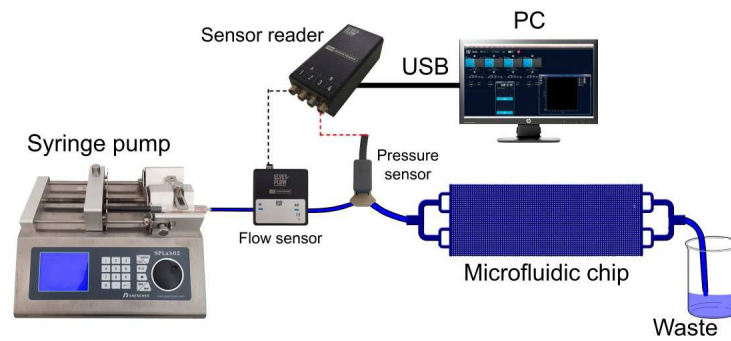


Fig. 3. Schematic diagram of the experimental microfluidic setup.

It is worth noting that the microchip fluid motion problems are characterized by very small flow velocities < 0.1 m/s, resulting in small Reynolds numbers $Re \leq 1$, which ensures a strictly laminar flow regime, the role of pipe friction loss is insignificant, therefore $\xi_\rho |q_i|^2 / 2f^2 = 0$. The values of the friction factor are determined by analytical formulas, for a round pipe $\lambda_{fr} = 64 / Re$, and for a rectangular pipe $\lambda_{fr} = 128 / (Re f(x))$, where x is the ratio of the sides of the pipe section, $f(x)$ is the first three terms of the series: $f(x) = 16/3 - 1024/\pi^5 x (\text{th}(\pi x/2) + \text{th}(3\pi x/2)/3^5 + \dots)$ [23]. Interrelation of the pressure field and flow rates can be done using the well proven SIMPLE-like algorithm [23].

A feature of this network model is that, in general, it does not depend on the network topology. The developed network algorithm, unlike most previously known ones, is universal and, in general, does not depend on the number of branches connected to one node. This is achieved due to the fact that in this network algorithm the connection between the flow and pressure fields in the network is carried out using a SIMPLE-like algorithm. This makes it possible to use common effective approaches to modeling 1D and 3D problems, including highly efficient solvers for systems of linear algebraic equations. The use of a single principle of connection between flow and pressure fields will make it possible to build hybrid 1D-3D models in which large spatial regions (such as caverns, fractures or supply channels) are modeled using 3D, and the channels connecting them using 1D models. Moreover, unlike most of the known hybrid models, in this algorithm it will be possible to obtain a continuous pressure field for the entire computational domain, due to the end-to-end solution of the pressure correction problem. Due to this, this network algorithm allows modeling very branched hydraulic networks. However, any new algorithm needs testing. Obtaining reliable experimental data for very extensive hydraulic networks is a very difficult task. In our work, very microfluidic chips containing more than 70 thousand connected channels were used to test network hydraulic algorithms and obtain experimental data. Earlier we have validated this approach for a large number of network fluid dynamics problems [13, 24, 25].

3.2 CFD methodology for a single-phase flow in microfluidic chip

To compare with the network simulation results, additional simulation was performed using computational fluid dynamics (CFD) methods. For this purpose, a system of Navier-Stokes equations was solved numerically. The problem was solved in three-dimensional stationary formulation. The range of flow rates, considered in the course of computations, was within the limits of laminar flow regime and corresponded to the conditions of conducted experiments.

In this case, the mass conservation equation has the standard form:

$$\nabla(\rho \cdot \vec{V}) = 0 \quad (5)$$

here ρ is the liquid density, \vec{V} is the velocity vector, determined by solving the momentum equation:

$$\nabla \cdot (\rho \cdot \vec{V} \vec{V}) = -\nabla p + \nabla \cdot [\mu (\nabla \vec{V})]. \quad (6)$$

The problem was solved in a three-dimensional stationary formulation. A pressure-based solver with double precision was used. To solve the system of non-linear differential equations (5-6) within the CFD approach, the standard finite volume method (FVM) was used [3]. The relationship between the velocity field and pressure was implemented using the SIMPLEC algorithm. The continuity balance was computed using the PRESTO scheme. A second order central difference scheme was used to approximate the convective terms of the Navier-Stokes equations. The AMG multigrid solver was used to solve systems of linear equations. The following boundary conditions were used to model the flow in microchannels: 1) the flow velocity was set at the inlet of the computational domain; 2) the Neumann conditions were specified at the outlet; 3) the no-slip condition was set on solid walls.

4. Methodology for Conducting Microfluidic Experiments to Validate the Network Model

To obtain data required for the validation of the developed network methodology, relevant to a single-phase flow, an experimental study of water flow regimes in fabricated microfluidic chips was carried out. A schematic diagram of the experimental setup is shown in Fig. 3.

The displacement fluid flow was controlled by a multi-channel high performance Elveflow OB1 MK3+ microfluidic pressure controller, which had two pressure channels designed for the ranges from 0 to 2 bar and from 0 to 8 bar. For the channel operating up to 8 bar the accuracy of maintaining pressure was 100 Pa, response time and pressure setting time was up to 9 and 35 ms, respectively, and minimum pressure increment was 24 Pa. Flow rate and pressure drop were monitored and controlled using ESI Microfluidic Software from Elveflow.

An external pressure source (compressor) is required to operate the controller. Compressed air from the pressure controller is supplied to a sealed reservoir with the displacing fluid to be tested. The microfluidic chip is connected to the reservoir by PTFE tubing with 1/16" outer diameter, and is positioned horizontally on the Peltier element heat stabilizer. From the top, the chip is covered with insulation for better temperature stabilization.

The MFS4 flow sensor, operating in the range from 0.03 to 1000 $\mu\text{l}/\text{min}$ with an accuracy of $\pm 5\%$ of the measured value was used. The response time of the sensor was up to 70 ms.



Pressure was recorded by a MPX5050GP relative pressure sensor with a measuring error of $\pm 2.5\%$. Operating temperature of the sensor ranged from -40 to $+125^\circ\text{C}$, operating pressure was up to 50 kPa.

During the experiments, the volumetric flow rate of the fluid at the inlet to the chip was varied, and the pressure drop in the microchip was measured against time. After the pressure drop has stabilized, an average pressure was taken for the set flow rate.

5. Numerical Simulation Results

5.1 Numerical simulation of a single-phase flow in a microfluidic chip with homogeneous permeability

Validation of the computational methodology was carried out by computing the water flow in microchips with different porous structures. The first validation was conducted for a microchip with a porous structure in the form of a grid consisting of $100\ \mu\text{m}$ wide channels, the chip height being $40\ \mu\text{m}$. The distance between the channels was $100\ \mu\text{m}$. The width and length of the computational domain were 7.5 and 20 mm, respectively. The geometry of the computational domain is shown in Fig. 4. The computational grid for CFD simulation included 5 million nodes. The computational grid was split with a uniform step in the XY plane. At least 10 partitioning nodes were set for each channel. According to the depth of the calculated area, a partition of 20 nodes was set. Methodological calculations have shown that a further detailing of the calculation grid is impractical, since it does not lead to a change in the calculation results by more than 1% . A fragment of the computational grid for CFD simulation is shown in Fig. 5. The problem was solved in a three-dimensional isothermal formulation. The computations were performed for water with density of $998\ \text{kg/m}^3$ and dynamic viscosity of $0.00098\ \text{Pa}\cdot\text{s}$. The flow velocity was set at the inlet of the computational domain, and the Neumann conditions were specified at the outlet (See Fig. 4a). The computations were performed in a wide range of flow rates from 25 to $400\ \mu\text{l/min}$. This range of flow rates corresponded to the Reynolds number range from 0.81 to 13 . The Reynolds number was determined by the formula $Re = \rho U d / \mu$, where $d = 4S / A$ - effective hydrodynamic diameter of the inlet channel into the microchip (S - channel cross-sectional area, A - channel section perimeter), U - inlet flow velocity. The computation results were compared with both experimental data obtained and network simulation data.

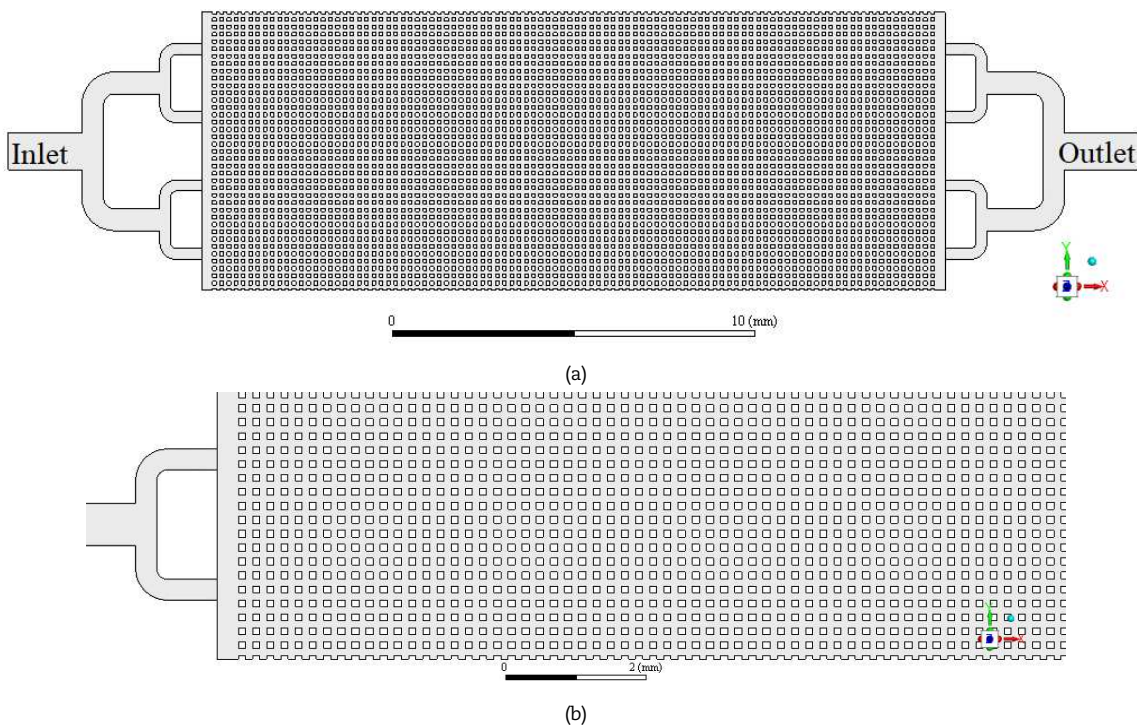


Fig. 4. Geometry of the computational domain for CFD simulation: (a) general view; (b) fragment at chip inlet.

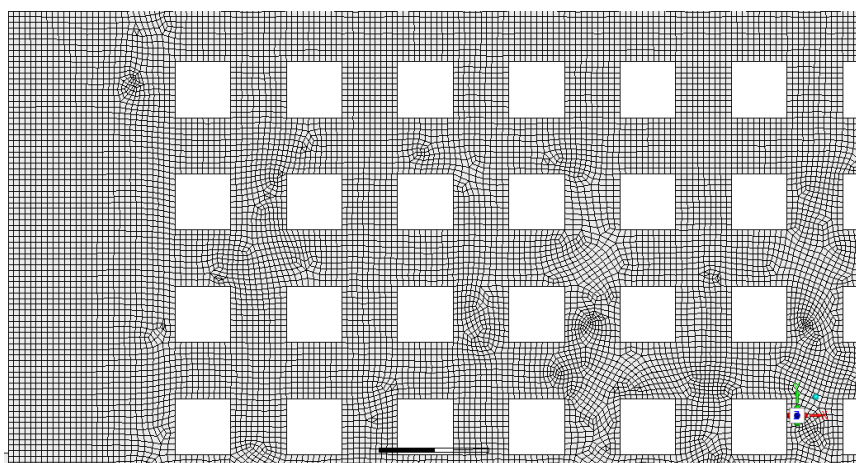


Fig. 5. Fragment of the computational grid for CFD simulation.



Table 1. Network model channel sizes.

# Groups	Quantity	Width, μm	Length, μm
1	2	1000	2000
2	4	600	4600
3	8	300	1800
4	152	300	50
5	7683	1000	1000

The same problem was also solved using network methods. A network model of the microchip with feeding channels consisting of 4128 nodes and 7849 branches was used (Fig. 6a). The height of the channels was set equal to $40\ \mu\text{m}$, the width and length depending on the position of the branch in the chip. All branches in the network model can be divided into 5 groups: the input/output channel, the first branch, the second branch, the channels of the distributing and prefabricated collectors, and the main channels of the lattice. The position of the channel groups is shown in the picture 6b, and the sizes and their number are shown in Table 1.

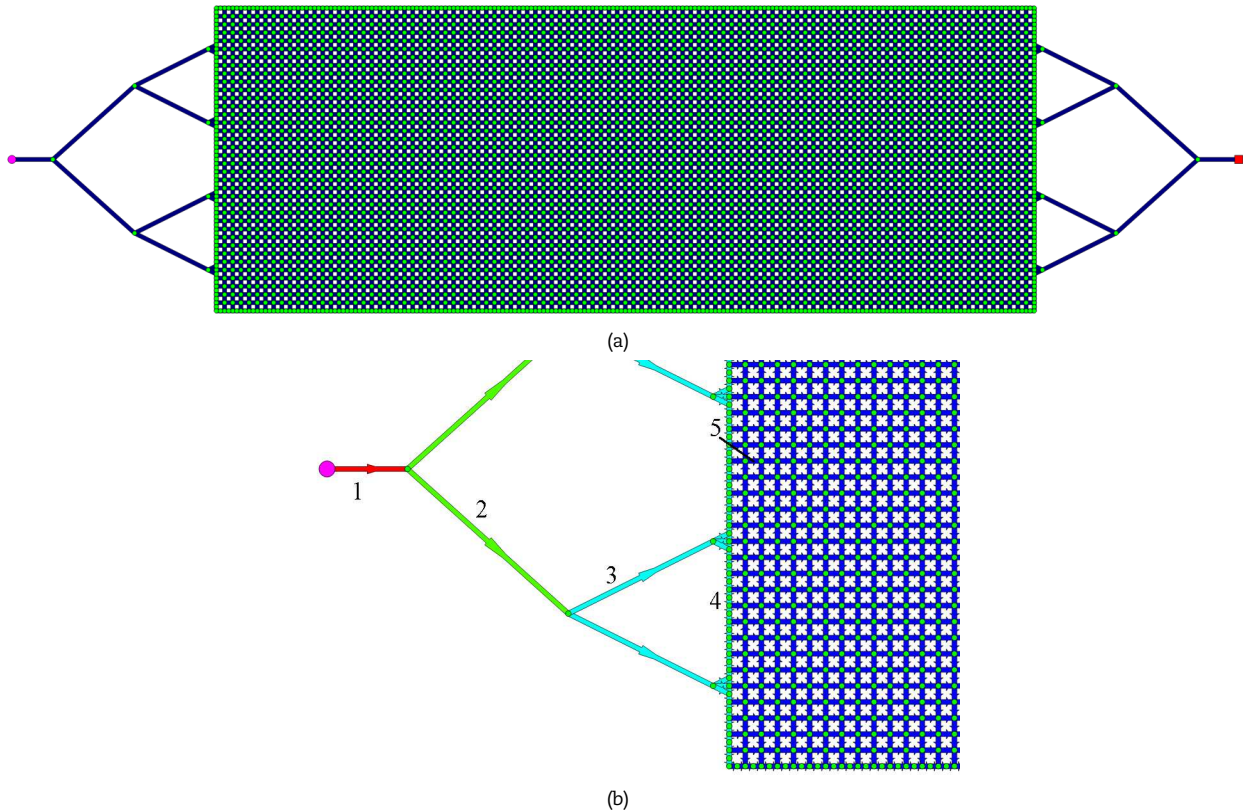


Fig. 6. Network model of the microchip: (a) microchip topology; (b) fragment of the inlet section of the chip.

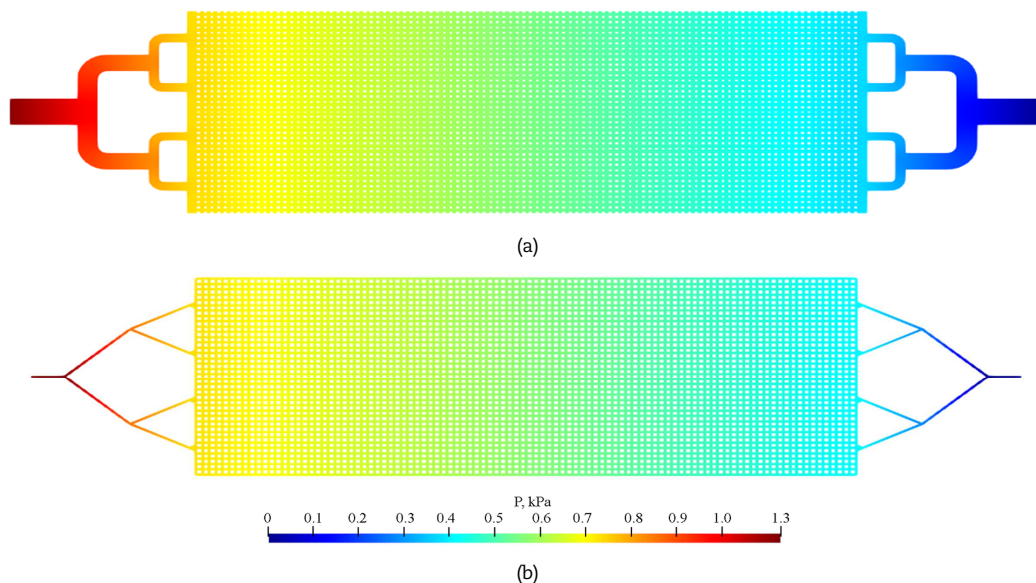


Fig. 7. Pressure field distribution: (a) in the CFD model; (b) in the network model.



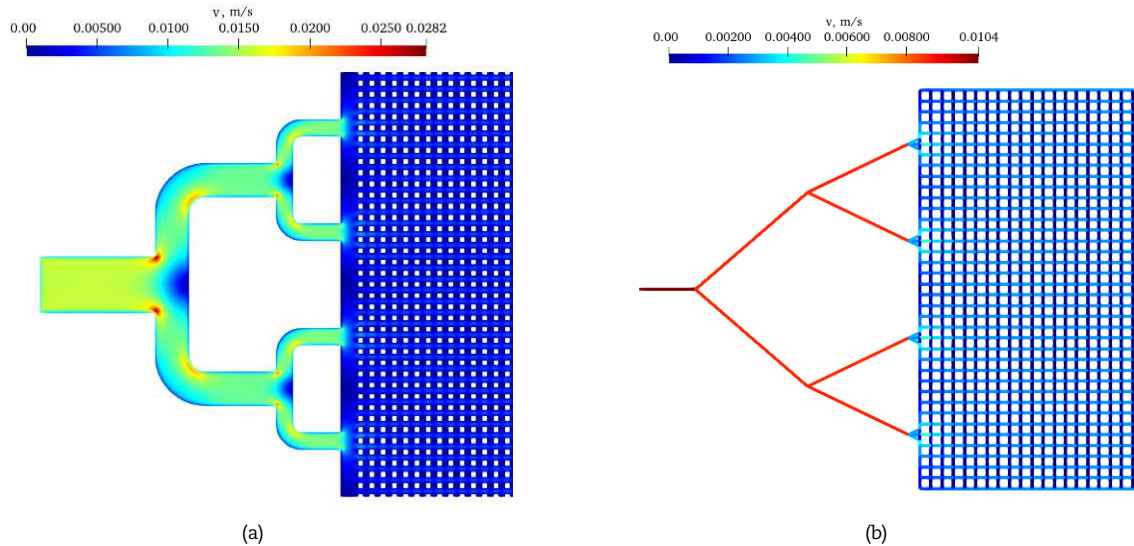


Fig. 8. Distribution of the local velocity field at the inlet section in the CFD model (a) and Distribution of cross-sectional average flow velocities at the inlet section in the network model (b).

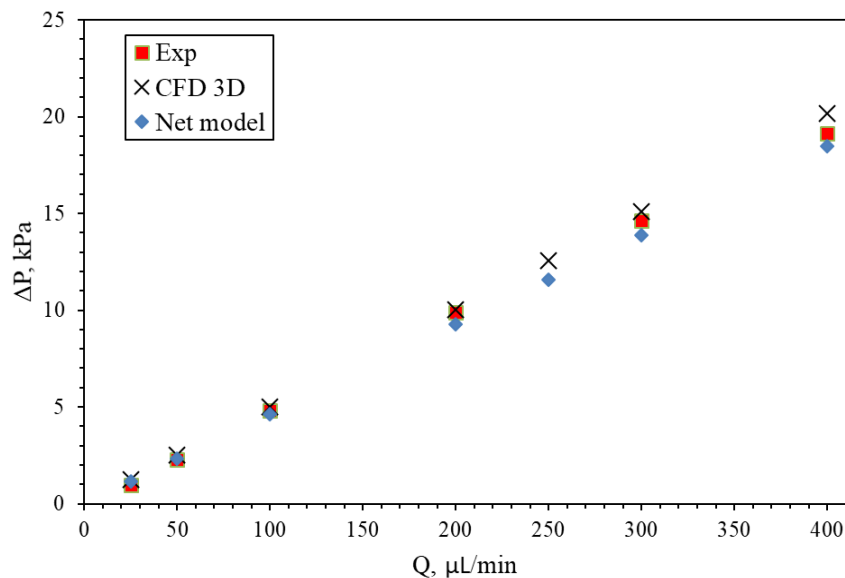


Fig. 9. Pressure drop depending on fluid flow rate.

In the course of conducted computations of single-phase flow in microchip with a regular grid of 100 μm , velocity and pressure distribution fields in porous medium, as well as pressure drops depending on liquid volumetric flow rate were obtained.

Velocity and pressure fields for volumetric flow rate of 25 $\mu\text{L}/\text{min}$ in both variants of the problem solution are shown in Figs. 7 and 8. It should be noted that Fig. 8a shows the local velocity field, in the central section of the way to the microchip, and Fig. 8b shows the average velocity values along the channel branches. Therefore, the maximum local speed is twice as high as the maximum average speed. This is evidenced by the color scale.

Analysis of simulation by both network and hydrodynamic models shows that the flow in the considered microfluidic chip is very homogeneous over the channel cross-section. Thus, the studied microfluidic chip can be considered as a very good approximation to the model of homogeneous porous medium. In general, there is a good qualitative concordance between two fundamentally different models describing such a flow.

Dependence of the pressure drop in the computational domain on liquid volumetric flow rate has been compared with obtained experimental data. Graphically this dependence is shown in Fig. 9. As can be seen from the graph, in the considered range, the pressure drop varies linearly with the flow rate. Hence, the main contribution to the flow resistance of the microchip is made by the linear friction resistance. At the same time, good agreement is seen between the calculated and experimental data in almost whole range of flow rates considered. Error analysis showed that the average error between the CFD model and the experiment is $\varepsilon_{\text{CFD_EXP}} = 4.3\%$, the average error between the Net model and the experiment is $\varepsilon_{\text{NET_EXP}} = 4\%$ and between different models is $\varepsilon_{\text{CFD_NET}} = 8\%$.

5.2 Numerical simulation of a single-phase flow in a microfluidic chip with heterogeneous permeability

The second verification-related problem was computing a single-phase isothermal flow in a microfluidic chip with heterogeneous permeability, consisting of four areas with channel sizes of 50 and 100 μm . The computational domain of porous medium was 15 mm wide and 40 mm long. The height of the microchip was 40 μm . The geometry of the computational domain is shown in Fig. 10.



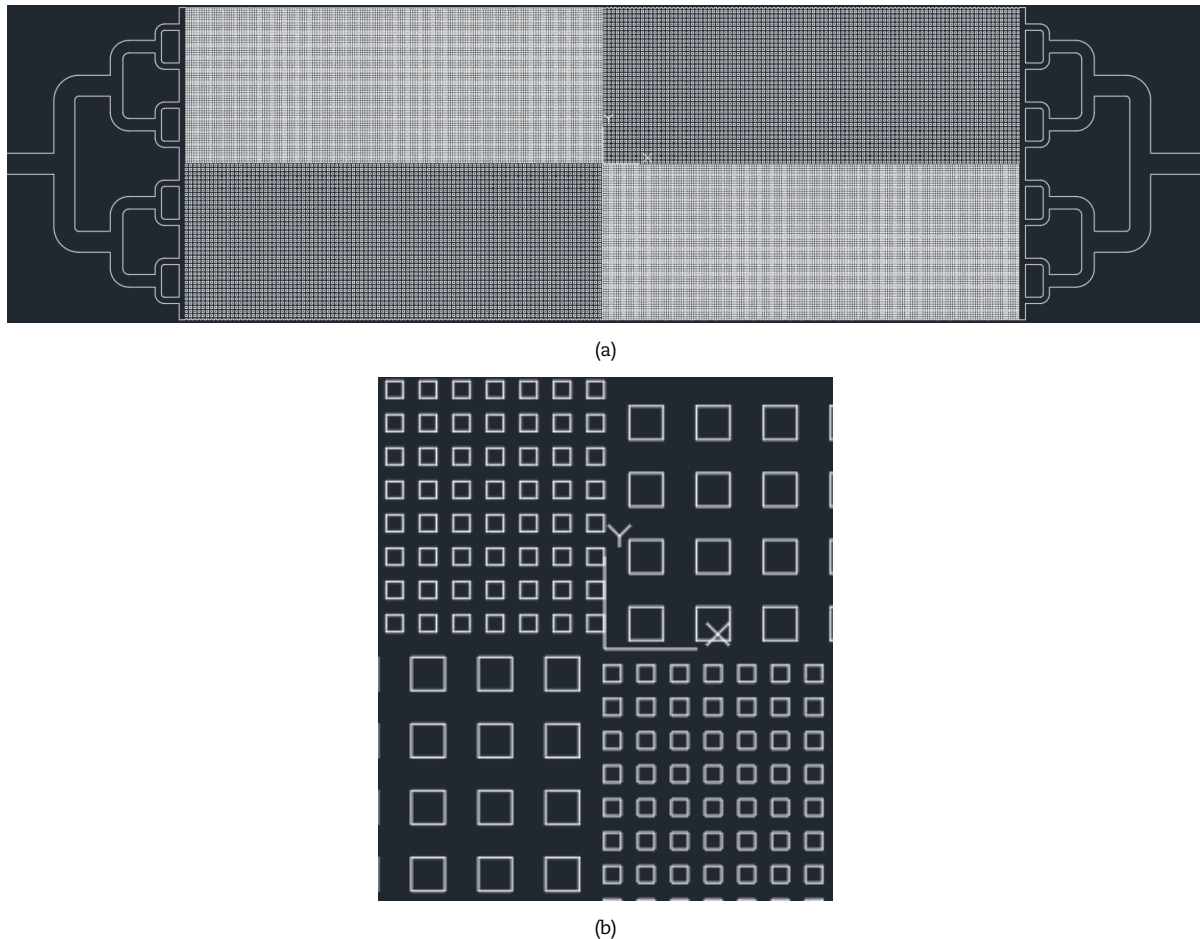


Fig. 10. Geometry of the computational domain for CFD simulation: (a) general view; (b) central part of the chip.

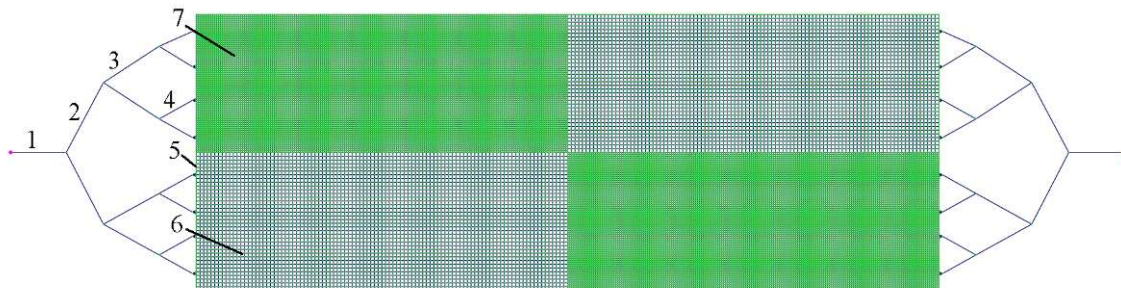


Fig. 11. Network model of a microchip with heterogeneous permeability.

The boundary conditions, set at the boundaries of the computational domain, were similar to those for the above described problem of a microchip with a channel size of $100\ \mu\text{m}$. The problem was solved in a three-dimensional isothermal formulation. The computations were performed for water with density of $998\ \text{kg/m}^3$ and dynamic viscosity of $0.00098\ \text{Pa}\cdot\text{s}$. The computations have been carried out over a wide range of flow rates from 25 to $400\ \mu\text{l/min}$. This range of flow rates corresponded to the Reynolds number range from 0.81 to 13. The Reynolds number was determined by the formula $Re = \rho U d / \mu$, where $d = 4S / A$ - effective hydrodynamic diameter of the inlet channel into the microchip (S - channel cross-sectional area, A - channel section perimeter), U - inlet flow velocity. The computation results were compared with both experimental data obtained and network simulation data.

The problem was solved in three dimensional (CFD) and network formulations. The computational grid for the CFD consisted of 16 million nodes. The computational grid was split with a uniform step in the XY plane. At least 12 partitioning nodes were set for each channel. According to the depth of the calculated area, a partition of 20 nodes was set. Methodological calculations have shown that a further detailing of the calculation grid is impractical, since it does not lead to a change in the calculation results by more than 1%. The network grid consisted of 37855 nodes and 74900 branches (see Fig. 11), and the sizes and their number are shown in Table 2.

The calculations produced pressure and velocity field distributions in the microchannel chip. A typical pressure field distribution (at flow rate of $100\ \mu\text{l/min}$) for both computation variants is shown in Fig. 12.



Table 2. Network model channel sizes.

#Groups	Quantity	Width, μm	Length, μm
1	2	1000	2000
2	4	1000	2000
3	8	600	4600
4	16	300	1800
5	608	300	50
6	15366	1000	1000
7	58896	500	500

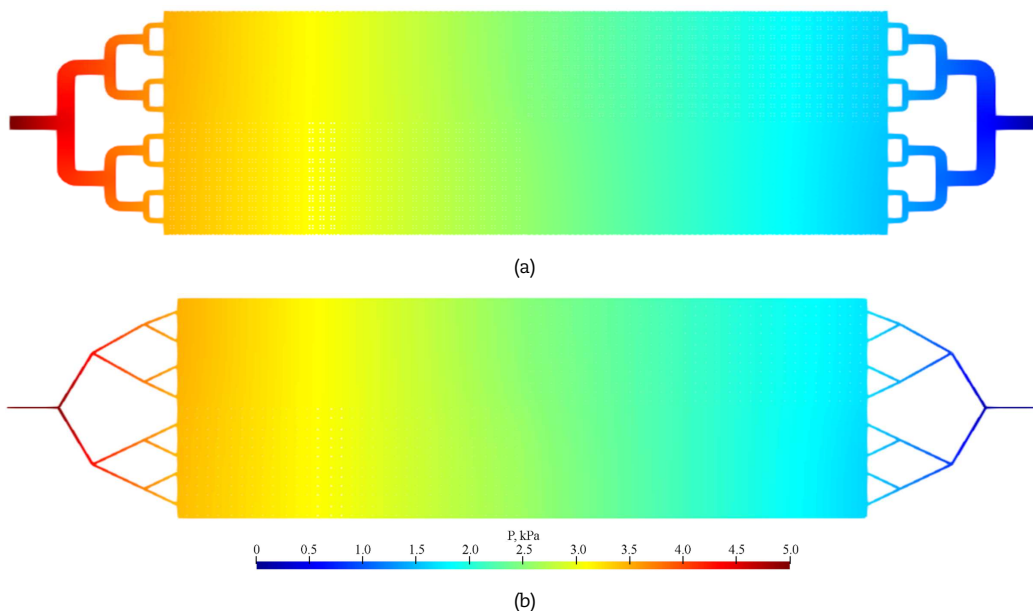


Fig. 12. Microchip pressure distribution at a flow rate of 100 $\mu\text{l}/\text{min}$: a) CFD model; b) network model.

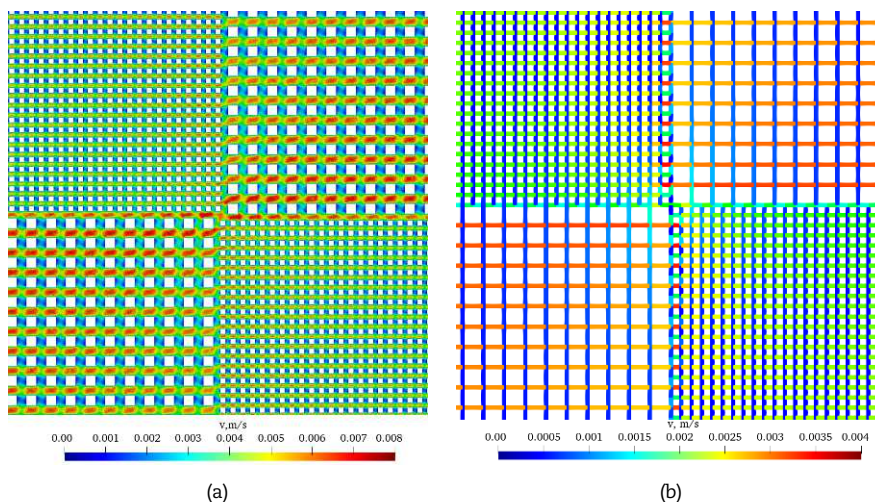


Fig. 13. Distribution of the local velocity field at the inlet section in the CFD model (a) and distribution of cross-sectional average flow velocities in the region of change in microchip permeability (b).

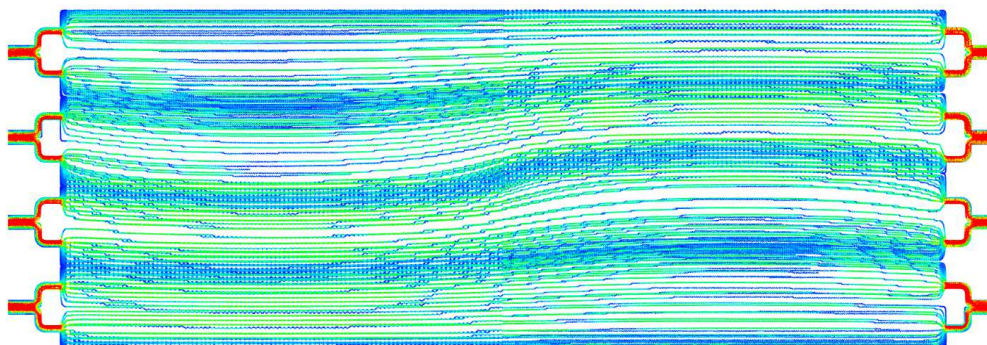


Fig. 14. Streamlines in the CFD model.



A comparison of the distribution patterns of the velocity field in the microchip channels with heterogeneous permeability, obtained using the CFD model and the network model, was carried out. Figure 13 shows the fluid flow in the area of change in the microchip permeability (local distribution of the velocity field (Fig. 13a) and the average velocity in the channels (Fig. 13b). At a distance from the central point, flow is observed only in horizontal channels, and there is practically no movement in vertical channels. When approaching the center of the microchip, the flow tends to move from the region of high permeability on the right to the region of high permeability on the left (or along the diagonal of the chip). In the network model, there is a significant increase in speed in vertical channels. This process is clearly visible with the help of streamlines, as a result of the calculation using the CFD model (Fig. 14).

As can be seen, the flow pattern differs significantly from the one discussed above for the homogeneous chip. The presence of a heterogeneous distribution of the hydraulic resistance of the channels causes the flow to be significantly redistributed. As a result, the main portion of the flow moves along the part of the microchip, which is formed by 100 μm channels. Having reached the junction with the area consisting of channels of 50 microns, the flow rearranges and moves again mainly in the area consisting of channels of 100 microns. This results in fact that in the microfluidic chip flow structure becomes S-shaped. The network simulation results reproduce qualitatively this flow feature very well. The flow patterns corresponding to the network and hydrodynamic simulations are in good agreement.

Quantitative comparison of computed data with experimental results was performed in terms of the dependence of pressure drop on flow rate, which is presented on Fig. 15.

From Fig. 15 it is evident, that computation results are in good agreement with data resulting from conducted experiments. The numerical technique for a single-phase flow regime quite accurately describes fluid flow in porous medium. The discrepancy between computed data and experimental results does not exceed 5% in the entire range of considered flow rates. It should be noted that in this case, the network simulation error is slightly higher than that in flow simulation in homogeneous chip. This is due to the fact that the network model does not take into account pressure losses at the junction of 100 and 50 μm channels. The CFD model-based computation shows that complex spatial flows form at such locations, which do not fit into the one-dimensional network simulation concept. For this reason, the network model calculation slightly underpredicts the overall pressure drop in the microfluidic chip. Error analysis showed that, $\epsilon_{CFD_EXP} = 4.8\%$, $\epsilon_{NET_EXP} = 4\%$, $\epsilon_{CFD_NET} = 2\%$. The decrease in the error between the two types of models is due to the fact that the influence of the input / output section of the microchip, in the simulation of which the main difference between the models is observed in the heterogeneous model is lower than in the homogeneous one.

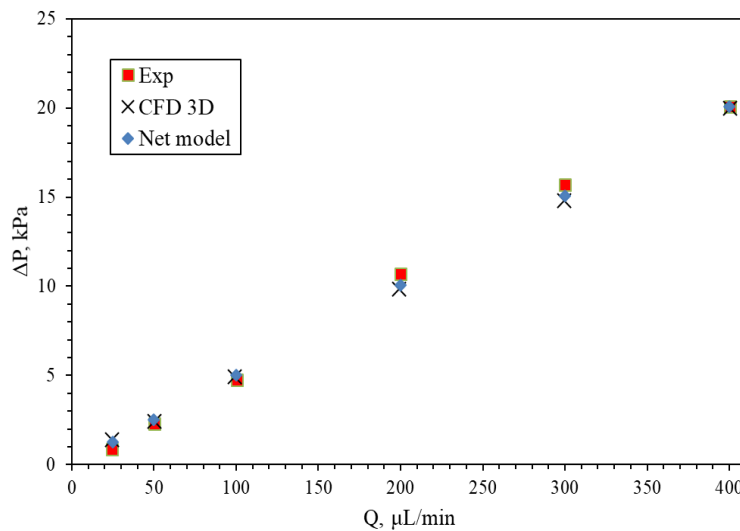


Fig. 15. Dependence of pressure drop on fluid flow rate.

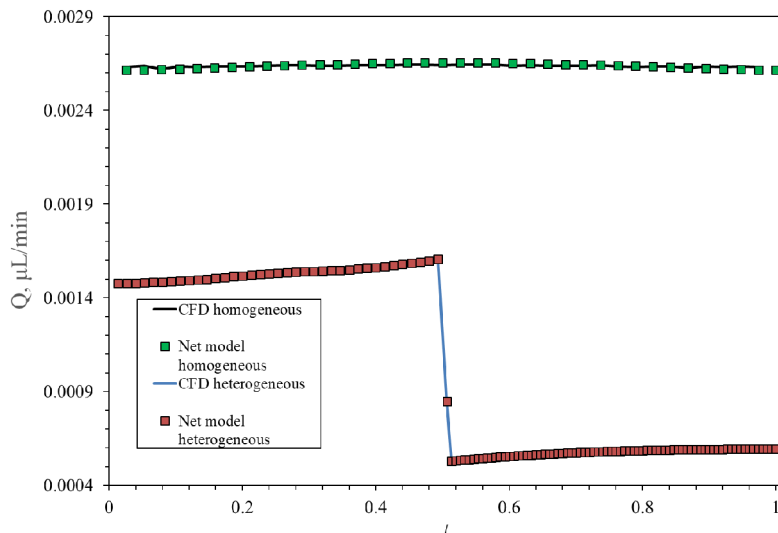


Fig. 16. Comparisons of local flow profiles in the cross section of microchips in network and CFD models.



Figure 16 shows the local flow distribution for both models in the cross section of microchips. The distributions are plotted in a section perpendicular to the flow, spaced from the entrance to the microchip by a distance equal to 20 mm. Along the OX axis, the distributions are dimensionless for the width of the section. For a homogeneous chip, it can be seen that the flow distribution is close to uniform with a slight decrease in flow towards the side walls of the chip. The maximum deviation in flow rates in the network and hydrodynamic models is 1.3%. For a heterogeneous microchip, the distribution is more complex. Most of the flow moves through half of the chip with wider channels and greater permeability. The flow rate in channels with higher permeability is about a factor of ten higher than in channels with lower permeability. The maximum discrepancy in the local flow distribution between the two models in this case is 5%.

The most important advantage of network models is their high performance compared to full CFD network fluid dynamics models. To demonstrate this advantage, estimates were made of the total time required to solve the flow problem in a heterogeneous chip using the network and hydrodynamic methods. Recall that to solve this problem using CFD method, a computational grid consisting of 16 million nodes was needed. Thus, 30 cores of AMD Ryzen Threadripper 3970X processor with 4000 MHz were used for computation. The time required to solve the problem for just one variant using CFD simulation was 1 hour. The time required to calculate the same variant using network simulation was just about one minute. Moreover, just one core of the same processor was used. Thus, the performance efficiency of network model is by 60 times more of magnitude higher than that for full hydrodynamic model when solving the same problem.

6. Conclusion

An original mathematical model and numerical algorithm for network computation of a single-phase flow in a highly branched pipeline chain have been developed. The network model, based on the approaches of the hydraulic circuit theory, provides a substantially higher computation speed as compared to CFD computational fluid dynamics methods. The numerical algorithm is based on the network analogue of the well-known control volume method. The essential difference of this work from others is that highly branched hydraulic networks with homogeneous and non-uniform permeability, containing more than 70 thousand branches, are considered. Such branched networks are important in many applications. Therefore, the development of algorithms for calculating flows in such networks is very important. In our work, to test network hydraulic algorithms, used microfluidic chips that were specially made for this purpose. A detailed verification and validation of the developed network algorithm was performed. For this purpose, microfluidic models of branched networks with homogeneous and heterogeneous permeability, containing several tens of thousands of branches were fabricated. Moreover, to verify the network model, CFD simulation data for full three-dimensional computation on the fine computational grids were used. Performed validation has shown a good qualitative and quantitative agreement between the results of network and hydrodynamic simulations, as well as with the data resulted from the conducted microfluidic experiments. The error of determining the total pressure drop in a branched hydraulic network with heterogeneous permeability, containing 37855 nodes and 74900 branches, was less than 5%. It has been shown that the performance efficiency of the network model is 60 times more of magnitude higher than that of the full hydrodynamic model provided quite close simulation accuracy. With a further increase in the number of channels in the hydraulic network this efficiency will nothing but increase. This makes it important to develop further network hydrodynamics methods.

Author Contributions

A.S. Yakimov made a micromodel chip. D.V. Guzei conducted numerical simulation and analyzed results, planned the scheme, review and editing; A.S. Filimonov developed the numerical algorithm for the network computation of a single-phase flow in a highly branched pipeline chain, review and editing; A.I. Pryazhnikov conducted the experiments and analyzed the empirical results; V.A. Zhigarev conducted numerical simulation; A.V. Minakov developed the mathematical modeling and examined the theory validation, review and editing. The manuscript was written through the contribution of all authors. All authors discussed the results, reviewed, and approved the final version of the manuscript.

Acknowledgments

The experimental data for validating the algorithm were obtained within the state assignment of the Ministry of Science and Higher Education of the Russian Federation (No. FSRZ-2020-0012).

Conflict of Interest

The authors declared no potential conflicts of interest concerning the research, authorship, and publication of this article.

Funding

The development of the network algorithm has been financially supported by the Russian Science Foundation within the project No. 23-79-30022, <https://rscf.ru/project/23-79-30022/>.

Data Availability Statements

The datasets generated and/or analyzed during the current study are available from the corresponding author on reasonable request.

Nomenclature

ρ	Density [kg/m ³]	q_i	Carrying flow in the branch [μ l/min]
\vec{v}	Velocity vector	Q_i	Mass source existing at the node [μ l/min]
λ_{fr}	Linear friction coefficient	p_{Di}	Pressure in the i -th node [kPa]
d	Hydraulic diameter of the branch [m]	P_c	Capillary pressure [kPa]
l	Branch length [m]	s_i	Drag coefficient



f	Pipe cross-section area [m ²]	u_i	Velocity on the i -th branch [m/s]
ξ	Local drag coefficient	N_{in}	Start node
O_i	Subset of branches starting at the i -th node	N_{out}	End node
I_i	Subset of branches ending at the i -th node		

References

- [1] Merenkov, A.P., Khasilev, V.Y., *Theory of Hydraulic Circuits*, Nauka, Moscow, 1985.
- [2] Novitsky, N.N., Tevyashev, A.D., *Pipeline systems of power engineering: Methodical and applied problems of simulation*, Nauka, Novosibirsk, 2015.
- [3] Todini, E., Santopietro, S., Gargano, R., Rossman, L.A., Pressure Flow-Based Algorithms for Pressure-Driven Analysis of Water Distribution Networks, *ASCE Journal of Water Resources Planning and Management*, 147(8), 2021, DOI: 10.1061/(ASCE)WR.1943-5452.0001401.
- [4] Wilson, R., *Introduction to Graph Theory*, Mir, Moscow, 1977
- [5] Singh, M., Mohanty, K.K., Dynamic modeling of drainage through three-dimensional porous materials, *Chemical Engineering Science*, 58(1), 2003, 1-18.
- [6] Regaieg, M., McDougall, S.R., Bondino, I., Hamon, G., Finger Thickening during Extra-Heavy Oil Waterflooding: Simulation and Interpretation Using Pore-Scale Modelling, *PLoS One*, 12(1), 2017, e0169727.
- [7] Aghaei, A., Piri, M., Direct pore-to-core up-scaling of displacement processes: Dynamic pore network modeling and experimentation, *Journal of Hydrology*, 522, 2015, 488-509.
- [8] Piri, M., Blunt, M.J., Three-dimensional mixed-wet random pore-scale network modeling of two- and three-phase flow in porous media. I. Model description, *Physical Review E*, 71(2), 2005, 026301.
- [9] Joeekar-Niasar, V., Hassanizadeh, S.M., Analysis of Fundamentals of Two-Phase Flow in Porous Media Using Dynamic Pore-Network Models: A Review, *Critical Reviews in Environmental Science and Technology*, 42(18), 2012, 1895-1976.
- [10] Filimonov, S.A., Pryazhnikov, M.I., Pryazhnikov, A.I., Minakov, A.V., Development and Testing of a Mathematical Model for Dynamic Network Simulation of the Oil Displacement Process, *Fluids*, 7(9), 2022, 311.
- [11] Lin, D., Hu, L., Bradford, S.A., Pore-network modeling of colloid transport and retention considering surface deposition, hydrodynamic bridging, and straining, *Journal of Hydrology*, 603(B), 2021, 127020.
- [12] Li, Z., Yang, H., Sun, Z., Espinoza, D.N., Balhoff, M.T., A Probability-Based Pore Network Model of Particle Jamming in Porous Media, *Transport in Porous Media*, 139(2), 2021, 419-445.
- [13] Filimonov, S.A., Dekterev A.A., Sentyabov, A.V., Minakov, A.V., Simulation of conjugate heat transfer in a microchannel system by a hybrid algorithm, *Journal of Applied and Industrial Mathematics*, 9(4), 2015, 469-479.
- [14] Weishaupt, K., Helmig, R., A Dynamic and Fully Implicit Non-Isothermal, Two-Phase, Two-Component Pore-Network Model Coupled to Single-Phase Free Flow for the Pore-Scale Description of Evaporation Processes, *Water Resources Research*, 57(4), 2021, e2020WR028772.
- [15] Zhao, J., Qin, F., Kang, Q., Derome, D., Carmeliet, J., Pore-scale simulation of drying in porous media using a hybrid lattice Boltzmann: pore network model, *Drying Technology An International Journal*, 40(4), 2022, 719-734.
- [16] Agaesse, T., Lamibrac, A., Buchi, F.N., Pauchet, J., Prat, M., Validation of pore network simulations of ex-situ water distributions in a gas diffusion layer of proton exchange membrane fuel cells with X-ray tomographic images, *Journal of Power Sources*, 331, 2016, 462-474.
- [17] Fani, M., Pourrafshary, P., Mostaghimi, P., Mosavat, N., Application of microfluidics in chemical enhanced oil recovery: A review, *Fuel*, 315, 2022, 123225.
- [18] Pryazhnikov, M.I., Minakov, A.V., Guzei, D.V., Yakimov, A.S., Flow Regimes Characteristics of Water-crude Oil in a Rectangular Y-microchannel, *Journal of Applied and Computational Mechanics*, 8(2), 2022, 655-670.
- [19] Lei, W., Liu, T., Xie, C., Yang, H., Wu, T., Wang, M., Enhanced oil recovery mechanism and recovery performance of micro-gel particle suspensions by microfluidic experiments, *Energy Science and Engineering*, 8, 2020, 986-998.
- [20] Al-Kharusi, A.S., Blunt, M.J., Network extraction from sandstone and carbonate pore space images, *Journal of Petroleum Science and Engineering*, 56(4), 2007, 219-231.
- [21] Raeini, A.Q., Bijeljic, B., Blunt, M.J., Generalized network modeling: Network extraction as a coarse-scale discretization of the void space of porous media, *Physical Review E*, 96(1), 2017, 013312.
- [22] Liu, Y., Gong, W., Zhao, Y., Jin, X., Wang, M., A pore-throat segmentation method based on local hydraulic resistance equivalence for pore-network modeling, *Water Resources Research*, 58, 2020, e2022WR033142.
- [23] Patankar, S.V., *Numerical heat transfer and fluid flow*, Series in computational methods in mechanics and thermal sciences, Hemisphere publishing corporation, Washington, 1980.
- [24] Filimonov, S.A., Neobyavlyayushchiy, P.A., Mikhienkova, E.I., An application of hybrid simulation algorithm for a research of the disposal system of noxious gases in aluminium production, *Vestnik Tomskogo Gosudarstvennogo Universiteta. Matematika i Mekhanika*, 44(6), 2016, 64-79.
- [25] Mikhienkova, E.I., Filimonov, S.A., Neobyavlyayushchiy, P.A., Boykov, D.V., Calculation of Industrial Enterprise Ventilation System by Network Integral Method, *MATEC Web of Conferences*, 72, 2016, 01070.

ORCID iD

S.A. Filimonov  <https://orcid.org/0000-0002-4044-3223>

D.V. Guzei  <https://orcid.org/0000-0003-2226-1837>

A.S. Yakimov  <https://orcid.org/0000-0003-4919-9877>

A.I. Pryazhnikov  <https://orcid.org/0000-0002-6124-037X>

V.A. Zhigarev  <https://orcid.org/0000-0001-5905-6365>

A.V. Minakov  <https://orcid.org/0000-0003-1956-5506>



© 2023 Shahid Chamran University of Ahvaz, Ahvaz, Iran. This article is an open access article distributed under the terms and conditions of the Creative Commons Attribution-NonCommercial 4.0 International (CC BY-NC 4.0 license) (<http://creativecommons.org/licenses/by-nc/4.0/>).

How to cite this article: Filimonov S.A., Guzei D.V., Yakimov A.S., Pryazhnikov A.I., Zhigarev V.A., Minakov A.V. Verification and Validation of a Network Algorithm for Single-phase Flow Modeling using Microfluidic Experiments, *J. Appl. Comput. Mech.*, 9(4), 2023, 1156-1167. <https://doi.org/10.22055/jacm.2023.43814.413>

Publisher's Note Shahid Chamran University of Ahvaz remains neutral with regard to jurisdictional claims in published maps and institutional affiliations.

